MSD Walls Technical Appendix v2.0.0

v2.0.0 Authors: J.J. Crispin, A.H. Bateman, Z. Struzik, E. Voyagaki, G. Mylonakis, and P.J. Vardanega

Released: February 2026

This technical appendix details the equations used in the python code available at: https://github.com/AbiBateman/MSD_Walls.

This code and technical appendix (v2.0.0) have been used in the publication:

Hua, Y., Struzik, Z., Bateman, A.H., Crispin, J.J., Huang, H., Zhang, D., Mylonakis, G.E. & Vardanega, P.J. (2026). Assessing the effectiveness of the mobilizable strength design method for prediction of retaining wall movements using a database, *submitted.*

v1.0.0 of this code and technical appendix have been used in the publication:

Crispin, J.J., Bateman, A.H., Voyagaki, E., Campbell, A., Mylonakis, G., Bolton, M.D. & Vardanega, P.J. (2024). MSD applied to the construction of the British Library basement: a multistage excavation in London Clay. *Canadian Geotechnical Journal*, 61(3):596-603. https://doi.org/10.1139/cgj-2023-0238

Section 1 of this supplement details the displacements from Stage 1 (pure rotation). Section 2 of this supplement details the displacements from the bulging stages (stages 2 onwards).

NOTATION

Latin

A = normalised (dimensional) parameter accounting for the potential energy loss at each stage (Eq. A6)
a = normalised (dimensionless) parameter accounting for the potential energy loss at each stage (Eq. A6)
B = normalised (dimensional) parameter accounting for the change in internal elastoplastic work (Eq. A7)
B_{max} = B normalised by the mobilisation factor (Eq. A14)
b = soil non-linearity exponent
b_0 = normalised (dimensionless) contribution to B of the constant component of s_u (Eq. A7)
b_{var} = normalised (dimensionless) contribution to B of the depth varying component of s_u (Eq. A7)
C_1, C_2 = normalised (dimensional) parameters used to describe the strain energy stored in the wall (Eq. A9)
EI = plane-strain bending stiffness per meter length of the wall
H_m = excavated depth at stage m
$H_{p,m}$ = depth to the prop installed prior to the excavation stage m
$h_{p,m}$ = distance between the excavated depth and the last installed prop [$h_{p,m} = H_m - H_{p,m}$]
L = length of the wall
M_c = similarity factor
m = excavation stage index
r = radial distance from the zone centre of rotation in zones CDE and EFH (Eq. A8)
r_0 = radial distance of the centre of rotation of zones CDE and EFH from point D (Eq. A8)
$r_{1,m} \approx 0.371\lambda_m$ = Radial distance from point D where the sign of $\delta\gamma$ changes in zone CDE
$r_{2,m}$, $r_{3,m}$ = two radial distances from point F where the sign of $\delta\gamma$ changes in zone EFH
r_p = radial distance from point F of peak value of $\delta\gamma$ in zone EFH
s_m = distance between the last installed prop and the base of the wall [$s_m = L - H_{p,m}$]
s_u = soil undrained shear strength
$s_{u,0}$ = soil undrained shear strength at the top of the wall
$s_{u,var}$ = change of the soil undrained shear strength per meter depth
w_m = wall displacement at excavation stage m
y = depth below the top of the wall

Greek

α_λ = modification factor to scale the displacement mechanism for different wall base conditions
β_m = soil strength mobilisation factor (τ/s_u) (Eq. A11)
γ = soil engineering shear strain
γ_{50} = soil shear strain when 50% of the soil shear strength is mobilised
$\gamma_{ave,m}$ = average mobilised shear strain in the mechanism for each stage m (Eq. A11)
γ_{sat} = soil saturated unit weight
ΔU_m = elastic strain energy stored in the wall at stage m
ΔP_m = potential energy loss at each stage m
ΔW_m = internal elastoplastic work at stage m
$\delta u_{y,m}$ = incremental vertical soil displacement at stage m
δw_m = incremental wall displacement at stage m
$\delta w_{max,m}$ = maximum incremental wall displacement at stage m (Eq. A1 & A10)
$\delta\gamma$ = incremental shear strain
$\delta\theta$ = angle of wall rotation during stage 1
λ_m = wavelength of the deformation mechanism
τ = soil engineering shear stress
χ_1 = contribution of the previous stages to β_m when $b = 0.5$ (Eq. A13b)
χ_2 = contribution of the current stage to β_m when $b = 0.5$ (Eq. A13c)

1. RIGID WALL ROTATION

Stage 1 of the excavation is modelled as pure rotation around the base of the wall (see Fig. A1). Triangular displacement mechanisms are modelled on both sides of the wall (Fig. A1). These deform in uniform shear (Osman & Bolton 2004) and energy equilibrium is considered (potential energy loss equals internal plastic work) to determine the wall rotation.

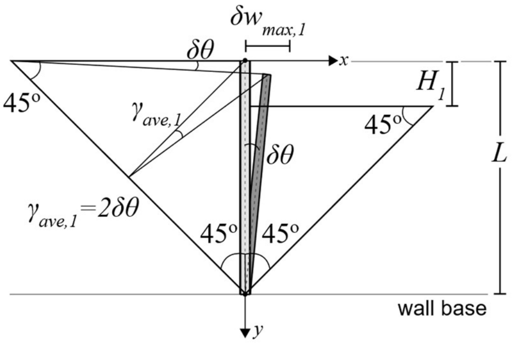

Figure A1. Illustration of the wall rotation around the base of the wall during stage 1 (modified from Osman & Bolton 2006).

By assuming a power-law soil constitutive model (Fig. A2a) and a linear variation of the shear strength, s_u, with depth below the top of the wall, y, ($s_u = s_{u,0} + s_{u,var}y$, see Fig. A2b), the following solution is obtained for the wall displacement at stage 1, δw_1 (modified from Osman & Bolton 2006).

$$\delta w_1 = \delta w_{max,1}\left(1-\frac{y}{L}\right) \tag{A1a}$$

$$\delta w_{max,1} = \frac{L\gamma_{50}}{2}\left[\frac{\gamma_{sat}H_1\left[3-3\left(\frac{H_1}{L}\right)+\left(\frac{H_1}{L}\right)^2\right]}{3s_{u,0}\left[2-2\left(\frac{H_1}{L}\right)+\left(\frac{H_1}{L}\right)^2\right]+s_{u,var}L\left[2-3\left(\frac{H_1}{L}\right)^2+2\left(\frac{H_1}{L}\right)^3\right]}\right]^{\frac{1}{b}} \tag{A1b}$$

where $\delta w_{max,1}$ is the maximum wall displacement at stage 1, L denotes the length of the wall, H_1 is the excavated depth at stage 1, γ_{sat} is the saturated unit weight of the soil, γ_{50} is the shear strain when 50% of the soil shear strength is mobilised, b is a soil non-linearity exponent, $s_{u,0}$ is the undrained shear strength at the surface of the soil and $s_{u,var}$ is the variation of the undrained shear strength with depth. The average mobilised shear strain in the mechanism $\gamma_{ave,1}$ is approximately twice the angle of rotation of the wall $\delta\theta$ [$\delta\theta = \delta w_{max,1}/L = \gamma_{ave,1}/2$].

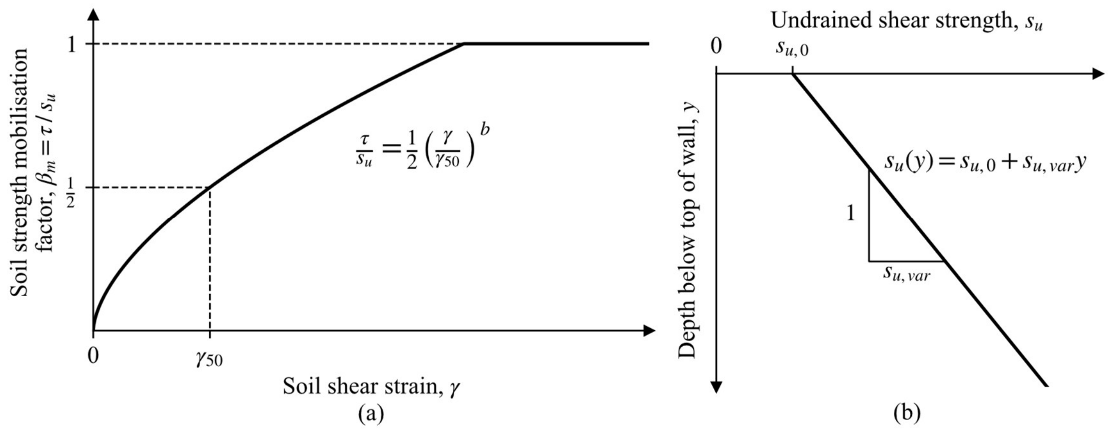

Figure A2. (a) Soil constitutive behaviour modelled using a power-law function (from Vardanega & Bolton 2011; note the bounds on this function from the original publication, $0.2 \leq \beta_m \leq 0.8$, it may not be valid outside of this range); (b) variation of soil undrained shear strength with depth

2. BULGING OF A BRACED EXCAVATION

An elastoplastic deformation mechanism, used by Osman & Bolton (2006), is assumed (depicted in Fig. A3). The wall, of length L, has a plane-strain bending stiffness per meter length of the wall EI. The wall has an assumed incremental displacement for each stage (for $m \geq 2$) according to the shape function (O'Rourke 1993):

$$\delta w_m(y) = \frac{1}{2}\left[1 - \cos\left(\frac{2\pi(y - H_{p,m})}{\lambda_m}\right)\right]\delta w_{max,m} \tag{A2}$$

where $\delta w_m(y)$ is the wall displacement as a function of the depth measured from the top of the wall y and $\delta w_{max,m}$ is the maximum wall displacement. Stage m refers to the current excavation stage, where H_m is the excavated depth, $H_{p,m}$ is the depth to the prop installed prior to this excavation stage. λ_m refers to the size of the deformation mechanism and is dependent on wall fixity at the base α_λ (shown in Fig. A3), given by:

$$\lambda_m = s_m \alpha_\lambda \tag{A3}$$

where s_m is the distance between the previously installed prop and the base of the wall [$s_m = L - H_{p,m}$] and α_λ is parameter used to model the boundary condition at the base of the wall (suggested by Osman & Bolton 2006).

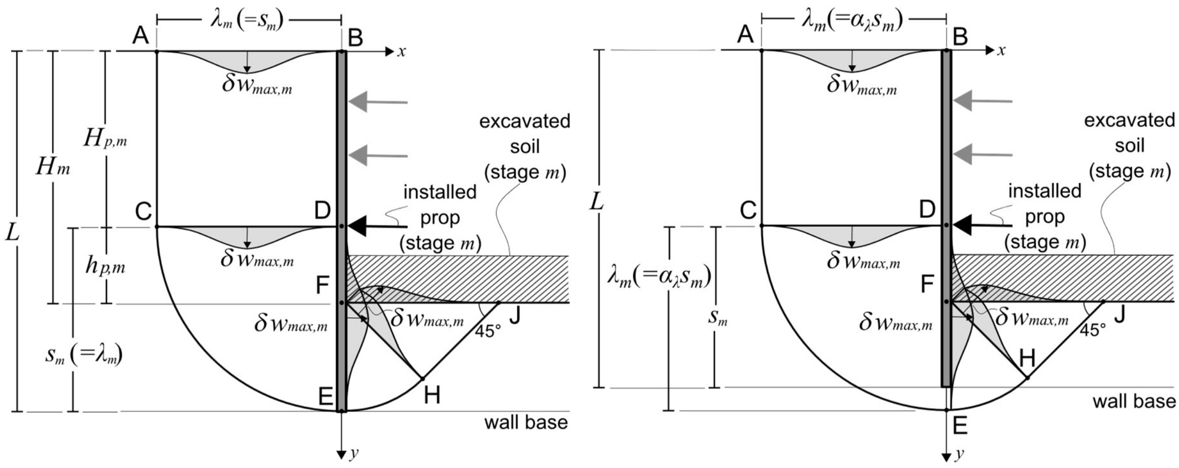

Figure A3. Incremental wall bulging at excavation stage m, plus plastic deformation mechanism considered for propped wall, for (a) $\alpha_\lambda = 1$, and (b) $\alpha_\lambda \approx 1.1$ (modified from Osman & Bolton 2006).

2.1 General Solution

Considering the above elastoplastic mechanism for each stage, the potential energy loss ΔP_m equals the sum of the internal elastoplastic work ΔW_m and the elastic strain energy stored in the wall ΔU_m (Lam & Bolton 2011):

$$\Delta P_m = \Delta W_m + \Delta U_m \tag{A4}$$

each term of which can be expressed as (modified from Lam & Bolton 2011):

$$\Delta P_m = \int_{area} \gamma_{sat}\, \delta u_{y,m}\, dArea \tag{A5a}$$

$$\Delta W_m = \int_{area} \left|\beta_m (s_{u,0} + s_{u,var} y)\delta\gamma\right|\, dArea \tag{A5b}$$

$$\Delta U_m = \frac{1}{2} EI \int_{H_{p,m}}^{L} \left[(\delta w_m'')^2 + 2\delta w_m'' \sum_{i=2}^{m-1} \delta w_i''\right] dy \tag{A5c}$$

where $\delta u_{y,m}$ is the incremental vertical soil displacement within the mechanism at each specific stage, $\delta\gamma$ is the corresponding incremental shear strain, β_m is the average mobilised stress within the mechanism (τ/s_u) defined by Vardanega & Bolton (2011), and y is the depth measured from the top of the wall. These equations are simplified from those provided in Lam & Bolton (2011) by removing the discretisation of the mechanism. Note these equations are for the bulging stages only (the sum in Eq. A5c starts at stage 2). Calculations for stage 1 (the rotation stage) are discussed in Section 1.

The potential energy loss ΔP_m (Eq. A5a) within the mechanism is given by:

$$\Delta P_m = A\delta w_{max,m} = [a\,\gamma_{sat}\lambda_m^2]\delta w_{max,m} \tag{A6}$$

where A and a are a normalised parameters (dimensional and dimensionless, respectively) used to describe the change in potential energy. The contribution to a for each zone within the mechanism is given in Table A1, where $h_{p,m}$ is the distance between the excavated depth and the last installed prop ($H_m - H_{p,m}$).

Table A1: Potential energy loss calculated for each zone within the mechanism

Zone	$\boldsymbol{a}$ **(Eq. A6)**
ABCD (rectangular)	$\overline{H_p}/2$
CDE (circular segment)	$1/4$
EFH (circular segment)	$-\left(\frac{2-\sqrt{2}}{8\pi^2}\right)\left[\pi^2\left(1-\overline{h_p}\right)^2 - \sin^2\left(\pi\,\overline{h_p}\right)\right]$
FHJ (triangular)	$-\frac{\sqrt{2}}{8\pi^2}\left[\pi^2\left(1-\overline{h_p}\right)^2 - \sin^2\left(\pi\,\overline{h_p}\right)\right]$
Total	$\frac{1}{4}\left[1+2\,\overline{H_p}-\left(1-\overline{h_p}\right)^2+\frac{1}{\pi^2}\sin^2\left(\pi\,\overline{h_p}\right)\right]$

$\overline{H_p} = H_{p,m}/\lambda_m$; $\overline{h_p} = h_{p,m}/\lambda_m$

Similarly, the internal elastoplastic work ΔW_m (Eq. A5b) within the mechanism is given by:

$$\Delta W_m = B\delta w_{max,m} = \beta_m B_{max}\delta w_{max,m} = \left[\beta_m\lambda_m\left(b_0 s_{u,0} + b_{var}\lambda_m s_{u,var}\right)\right]\delta w_{max,m} \tag{A7}$$

where b_0 and b_{var} are the (dimensionless) contributions due to the constant and depth varying components of s_u, respectively. B is a normalised (dimensional) parameter used to describe the change in internal elastoplastic work and B_{max} is B normalised by the mobilisation factor, $\beta_m = \tau/s_u$ (Eq. A11a). The contribution to B for each zone within the mechanism is split into b_0 and b_{var} as given in Table A2 and A3, respectively.

Note that Eq. A5b requires the absolute value of the virtual strain, $\delta\gamma$. Therefore, for zones CDE and EFH, where $\delta\gamma$ can change sign, the integrated function is no-longer continuous, and the integration must be split into sub-zones. Changes in sign can be found from the roots of $\delta\gamma(r)$, where r is the radial distance from the zone centre of rotation. For zone CDE, this occurs at $r = r_{1,m} \approx 0.371\lambda_m$, where r is the distance from point D. For EFH, a sign change only occurs when $h_{p,m}$ is below approximately $0.091\lambda_m$, or, more accurately, when the peak value of $\delta\gamma$ (at radius r_p from point F) is positive. r_p is in turn found from the root of $d\delta\gamma(r)/dr$, the derivative of $\delta\gamma$

with respect to r. If $\delta\gamma(r_p) > 0$, there are two sign changes, at $r = r_{2,m}$ and $r = r_{3,m}$. Values for r_p, $r_{1,m}$, $r_{2,m}$ and $r_{3,m}$ can be obtained through numerical root finding methods, such as bisection, using the following equations:

$$\delta\gamma(r) = \frac{\pi}{\lambda_m}\sin\left(2\pi\frac{r+r_0}{\lambda_m}\right) - \frac{1}{2r}\left(1-\cos\left(2\pi\frac{r+r_0}{\lambda_m}\right)\right) \quad \text{(A8a)}$$

$$\frac{d\delta\gamma(r)}{dr} = \frac{1}{2r^2}\left[1-\left(1-4\pi^2\frac{r^2}{\lambda_m^2}\right)\cos\left(2\pi\frac{r+r_0}{\lambda_m}\right) - 2\pi\frac{r}{\lambda_m}\sin\left(2\pi\frac{r+r_0}{\lambda_m}\right)\right] \quad \text{(A8b)}$$

where r_0 is the distance of the centre of rotation from point D. $r_0 = 0$ for zone CDE, and $r_0 = h_{p,m}$ for zone EFH.

Table A2: Internal elastoplastic work calculated for each zone within the mechanism

Zone	$\boldsymbol{b_0}$ **(Eq. A7)**
ABCD (rectangular)	$2\,\overline{H_p}$
CDE (circular segment)	$\frac{1}{2}[\sin(2\pi\,\overline{r_1}) - 2\pi\,\overline{r_1}\cos^2(\pi\,\overline{r_1}) + \pi]$ where $\overline{r_1} \approx 0.371$ (see above Eq. A8)
EFH (circular segment)	if $\delta\gamma(r_p) \le 0$: (approximately $\overline{h_p} > 0.091$) $\frac{1}{8}\left[\sin(2\pi\,\overline{h_p}) - 2\pi(\overline{h_p}-1)\right]$ else: $\frac{1}{8}\Big[2\pi(1-\overline{h_p}) + \sin(2\pi\overline{h_p})$ $+2\sin\left(2\pi(\overline{h_p}+\overline{r_3})\right) - 2\sin\left(2\pi\left(\overline{h_p}+\overline{r_2}\right)\right)$ $+2\pi\overline{r_2}\left(\cos\left(2\pi\left(\overline{h_p}+\overline{r_2}\right)\right)+1\right) - 2\pi\overline{r_3}\left(\cos\left(2\pi(\overline{h_p}+\overline{r_3})\right)+1\right)\Big]$ where r_p, $\overline{r_2}$ and $\overline{r_3}$ can be obtained from the method described above Eq. A8
FHJ (triangular)	$\frac{1}{4\pi}\left[4\pi - \sin(2\pi\,\overline{h_p}) - 6\pi\,\overline{h_p}\right]$

where $\overline{H_p} = H_{p,m}/\lambda_m$; $\overline{h_p} = h_{p,m}/\lambda_m$; $\overline{r_1} = r_{1,m}/\lambda_m$; $\overline{r_2} = r_{2,m}/\lambda_m$; $\overline{r_3} = r_{3,m}/\lambda_m$

Table A3: Internal elastoplastic work calculated for each zone within the mechanism

Zone	$\boldsymbol{b_{var}}$ **(Eq. A7)**
ABCD (rectangular)	$\overline{H_p}^2$
CDE (circular segment)	$\frac{1}{4\pi^2}\left[6\pi\,\overline{r_1}\sin(2\pi\,\overline{r_1}) - 3(1-\cos(2\pi\,\overline{r_1})) + \pi^2(3 - 4\,\overline{r_1}^2\cos(2\pi\,\overline{r_1}) - 2\,\overline{r_1}^2) + 2\pi^2\overline{H_p}(\pi - \pi\,\overline{r_1}(1+\cos(2\pi\,\overline{r_1})) + \sin(2\pi\,\overline{r_1}))\right]$ where $\overline{r_1} \approx 0.371$ (see above Eq. A8)
EFH (circular segment)	if $\delta\gamma\left(r_p\right) \le 0$: (approximately $\overline{h_p} > 0.091$) $\frac{1}{16\pi^2}\left[3\sqrt{2}\left(\cos\left(2\pi\,\overline{h_p}\right)-1\right) + 4\pi^3\overline{H}\left(1-\overline{h_p}\right) + 2\pi^2\left(\overline{H}\sin\left(2\pi\,\overline{h_p}\right) + 3\sqrt{2}\left(1-\overline{h_p}\right)^2\right)\right]$ else: $\frac{1}{16\pi^2}\left[2\sqrt{2}\pi^2\left(2\,\overline{r_2}^2 - 2\,\overline{r_3^2} + 3\left(1-\overline{h_p}\right)^2\right) + 4\pi^3\overline{H}\left(1-\overline{h_p}+\overline{r_2}-\overline{r_3}\right) - 3\sqrt{2} + 3\sqrt{2}\left(\cos\left(2\pi\,\overline{h_p}\right) - 2(c_{r2}-c_{r3})\right) + 2\pi^2\overline{H}\left(\sin\left(2\pi\,\overline{h_p}\right) - 2(s_{r2}-s_{r3})\right) + 4\pi^3\overline{H}(\overline{r_2}c_{r2} - \overline{r_3}c_{r3}) - 12\sqrt{2}\pi(\overline{r_2}s_{r2} - \overline{r_3}s_{r3}) + 8\sqrt{2}\pi^2(\overline{r_2}^2c_{r2} - \overline{r_3}^2c_{r3})\right]$ where c_{r2}, c_{r3}, s_{r2} and s_{r3} are given by: $c_{r2} = \cos\left(2\pi\left(\overline{h_p}+\overline{r_2}\right)\right)$; $c_{r3} = \cos\left(2\pi\left(\overline{h_p}+\overline{r_3}\right)\right)$ $s_{r2} = \sin\left(2\pi\left(\overline{h_p}+\overline{r_2}\right)\right)$; $s_{r3} = \sin\left(2\pi\left(\overline{h_p}+\overline{r_3}\right)\right)$ and r_p, $\overline{r_2}$ and $\overline{r_3}$ can be obtained from the method described above Eq. A8
FHJ (triangular)	$\frac{1}{16\pi^2}\left[\pi^2\left(3\sqrt{2} + 16\overline{H} - 24\overline{h_p}\,\overline{H} + 6\sqrt{2}\,\overline{h_p}^2 - 8\sqrt{2}\,\overline{h_p}\right) - 4\pi\overline{H}\sin(2\pi\overline{h_p}) - 2\sqrt{2}\left(\cos^2(\pi\overline{h_p}) + 1\right)\right]$

where $\overline{H_p} = H_{p,m}/\lambda_m$; $\overline{H} = H_m/\lambda_m$; $\overline{h_p} = h_{p,m}/\lambda_m$; $\overline{r_1} = r_{1,m}/\lambda_m$; $\overline{r_2} = r_{2,m}/\lambda_m$; $\overline{r_3} = r_{3,m}/\lambda_m$

Finally, the elastic strain energy stored in the wall ΔU_m (Eq. A5c) can be calculated as:

$$\Delta U_m = C_1\,\delta w_{max,m}^2 + C_2\,\delta w_{max,m} \tag{A9a}$$

$$C_1 = \pi^4\frac{EI}{\lambda_m^3}\left[\frac{1}{\alpha_\lambda} + \frac{1}{4\pi}\sin\left(\frac{4\pi}{\alpha_\lambda}\right)\right] \tag{A9b}$$

$$C_2 = \pi^3 EI\sum_{i=2}^{m-1}\frac{\delta w_{max,i}}{\lambda_i^3\left(1+\frac{\lambda_m}{\lambda_i}\right)}\left[\frac{2}{\frac{\lambda_m}{\lambda_i}-1}\sin\left(\frac{2\pi}{\alpha_\lambda}\left(\frac{\lambda_m}{\lambda_i}-1\right)\right) + \frac{\lambda_i}{\lambda_m}\sin\left(\frac{4\pi}{\alpha_\lambda}\right)\right] \tag{A9c}$$

where C_1 and C_2 are normalised (dimensional) parameters used to describe the strain energy stored in the wall.

Substituting Eqs. A6, A7 and A9 into Eq. A4 yields:

$$\delta w_{max,m} = \frac{A-B-C_2}{C_1} \tag{A10}$$

The above solution requires assuming a value for the mobilisation factor β_m contributing to coefficient B. The soil shear stress mobilisation factor β_m can be found using the assumed soil constitutive model (Fig A2(a)) and setting the shear strain to average shear strain in the mechanism for each stage, $\gamma_{ave,m}$:

$$\beta_m = \frac{\tau}{s_u} = \frac{1}{2}\left(\frac{\gamma_{ave,m}}{\gamma_{50}}\right)^b \tag{A11a}$$

The average shear strain in the mechanism can be calculated as (Lam & Bolton 2011):

$$\gamma_{ave,m} = M_c \sum_{i=2}^{m} \frac{\delta w_{max,i}}{\lambda_i} \tag{A11b}$$

where M_c is a similarity factor suggested by Osman & Bolton (2006) to be 2.0 ($\pm$10%).

Eq. A10 is a polynomial of $\delta w_{max,m}$. When $b \neq 0.5$ (as per the example in the main text) an iterative approach is suggested to find a solution. In the supplied spreadsheet, a “guess” can be changed manually until it matches the predicted (“result”) incremental maximum displacement within a tolerable error. This is automated in the provided python script.

The overall displacements (for $m \geq 2$) can then be found by superimposing the displacements along the wall for each stage, including the rotation stage, Eq. A1a (Clough *et al.* 1989):

$$w_m = \delta w_{max,1}\left(1 - \frac{y}{L}\right) + \sum_{i=2}^{m} \frac{1}{2}\left[1 - \cos\left(\frac{2\pi(y - H_{p,m})}{\lambda_m}\right)\right] \delta w_{max,m} \tag{A12}$$

2.2 Closed Form Solution (*b = 0.5*)

For the special case where $b = 0.5$, a closed-form solution can be derived that allows solving directly for $\delta w_{max,m}$ without iteration (as is required for the above general solution). Using this assumption, β_m can be written as:

$$\beta_m = \frac{1}{2}\sqrt{\chi_1 + \chi_2 \delta w_{max,m}} \tag{A13a}$$

$$\chi_1 = \frac{M_c}{4\gamma_{50}} \sum_{i=1}^{m-1} \frac{\delta w_{max,i}}{\lambda_i} \tag{A13b}$$

$$\chi_2 = \frac{M_c}{4\lambda_m \gamma_{50}} \tag{A13c}$$

where χ_1 and χ_2 are the contributions of the previous and current stages, respectively, to β_m.

Then, substituting Eqs. A6, A7, A9 and A13 into Eq. A4 yields:

$$\delta w_{max,m} = \frac{1}{2C_1^2}\left[B_{max}^2 \chi_2 + 2C_1(A - C_2) - B_{max}\sqrt{B_{max}^2 \chi_2^2 + 4\chi_2 C_1 A + 4\chi_1 C_1^2 - 4\chi_2 C_1 C_2}\right] \tag{A14}$$

REFERENCES

Clough, G.W., Smith, E.M. & Sweeney, B.P. (1989). Movement control of excavation support systems by iterative design. *Proceedings of the ASCE Foundation Engineering*, ASCE. 1, 869–884.

Lam, S.Y. & Bolton, M.D. (2011). Energy conservation as a principle underlying mobilizable strength design for deep excavations. *Journal of Geotechnical and Geoenvironmental Engineering, ASCE*, 137(11): 1062-1074. https://doi.org/10.1061/(ASCE)GT.1943-5606.0000510

O’Rourke, T.D. (1993). Base stability and ground movement prediction for excavations in soft clay. In Retaining structures (pp. 657–686). Thomas Telford Publishing.

Osman, A.S. & Bolton, M.D. (2004). A new design method for retaining walls in clay. *Canadian Geotechnical Journal*, 41(3), 451–466. https://doi.org/10.1139/t04-003

Osman, A.S. & Bolton, M.D. (2006). Ground movement predictions for braced excavations in undrained clay. *Journal of Geotechnical and Geoenvironmental Engineering*, ASCE, 132(4): 465-477. https://doi.org/10.1061/(ASCE)1090-0241(2006)132:4(465)

Vardanega, P.J. & Bolton, M.D. (2011). Strength mobilization in clays and silts. *Canadian Geotechnical Journal*, 48(10), 1485-1503, http://doi.org/10.1139/T11-052 [corrigendum, 49(5), 631, http://doi.org/10.1139/t2012-023].